Desalination and Water Treatment
www.deswater.com

doi: 10.5004/dwt.2018.22728

124 (2018) 308–318
August

Synthesis and characterization of TiO_2 nanoparticles loaded activated carbon for Congo Red removal from wastewater: kinetic and equilibrium studies

Ahmad Azari[a,*], Rezvan Rezaei[a], Hamidreza Sanaeepur[b]

[a]*Faculty of Petroleum, Gas and Petrochemical Engineering (FPGPE), Persian Gulf University (PGU), P.O. Box 75169-13817, Bushehr, Iran, email: azari.ahmad@pgu.ac.ir (A. Azari), Tel. +98 773122 2616, Fax +98 73344 5182, email: r_rezaei_r@yahoo.com (R. Rezaei)*
[b]*Department of Chemical Engineering, Faculty of Engineering, Arak University, Arak 38156-8-8349, Iran, email: h.sanaee@yahoo.com, h-sanaeepur@araku.ac.ir (H. Sanaeepur)*

Received 17 September 2017; Accepted 12 July 2018

ABSTRACT

Activated carbon (AC) was impregnated with titanium dioxide (TiO_2) to synthesize AC/TiO_2 nanocomposite through the sol-gel method at 400°C. Nanocomposite characterization was conducted by XRD, SEM and FTIR analyses. The synthesized nanoparticles were phase-pure anatase nanocrystallites with the average size of 10 nm. The AC/TiO_2 nanocomposites were applied for the first time to photocatalytic decomposition of Congo red (CR) dye under ultraviolet (UV) irradiation in a photoreactor. The effects of AC/TiO_2 nanocatalyst dosage (0.3–1 g), CR concentration (20–100 ppm), pH (3–9) and temperature (30–50°C) were examined for removal of CR solution pigments. Moreover, the adsorption kinetics and isotherm models were investigated on the AC and synthesized AC/TiO_2 nanophotocatalyst. The adsorption mechanism was found to be a pseudo-second-order kinetics with the good agreement for both adsorbents. Also the experimental isotherms were appropriately described by the Langmuir and Temkin models for AC adsorbent and AC/TiO_2 nanocomposite, respectively.

Keywords: Photocatalysts; Congo red; Titanium dioxide; Activated carbon; Nanocomposites

1. Introduction

Dyes are widely utilized in various industrial activities such as textiles, coloring, paper, leather, plastics, cosmetics and food. Their complex (aromatic) molecular structures lead to an increase in their resistance to heat, oxidizing agents and biodegradation. Toxicity of most dyes makes them harmful for some microorganisms and decreases severely their catalytic activity. However, the toxicity of dyes on plant, animal and human health is not well-known [1]. The dyes according to their charge divided to some categories such as acidic, basic, disperse, azo and diazo [2]. Congo red (CR) is an example of diazo dyes and is prepared by coupling tetrazotised benzidine with two molecules of napthionic acid. This is red in the pH range of 5–10, and its sodium salt dyes cotton full red [3]. Congo red is the first synthetic dye produced that is capable of dying cotton directly. It is very sensitive to acids and the color changes from red to blue in the presence of inorganic acids (below pH 5). This blue color may be attributed to resonance among charged canonical structures [3]. CR containing effluents are generated from textiles, printing and dyeing, paper, rubber, plastics industries, etc. Due to its structural stability, it is difficult to biodegrade [4]. These days approximately a million metric tons of dyes are produced annually in the world of azo dyes (R1-N=N-R2), which is signify about 72% of the total dyes [5]. According to the recent survey, about two third of its market are being used in textile industries [6]. It has been indicated that 14% of the non natural textile dyes used every year are disposed off to water streams. Waste water treatment plants are the major sources of the addition of these to the environment. Due to the stability and complexity in structure of dyes, it is very difficult to decolorize dyes, which make it compulsory to get rid of

*Corresponding author.

them from industrial sewages before disposing them off into the main stream [7]. The effluent from a dye industry usually contains 0.5–0.8 g dye/L [8].

Anionic dyes are highly water soluble and generate serious problems, namely mutagenic and carcinogenic activities, therefore it is necessary to remove these dyes [9]. The treatment of textile waste waters in order to diminish visual colors and dissolved organic contaminants is an attractive field of interest for researchers. The non-degradable nature and the high stability towards light and oxidizing agents are barriers for the selection of suitable methods for treatment of textile waste waters. Among the diverse dye treatment technologies, adsorption is the most versatile and widely applicable method because of its ability for separation of a wide range of chemical compounds with simple operational procedures [10–14].

Nowadays, nanomaterials with special physicochemical properties (high surface areas) are repeatedly applied for removal of large amounts of pollutants in a short reasonable time. The use of nanoparticles in various fields due to their size and surface structure was increased [15]. Activated carbon (AC) is known as the most widely used adsorbent due to its high adsorption area, low cost and simple regeneration. Its adsorption capacity is strongly affected by many variables, including its physical nature, functional groups, ash content and also by the nature of the adsorbate [16].

Titanium dioxide (TiO_2) is a chemically and biologically inert, photoactive and inexpensive material which is frequently used as the photocatalytic support in production of wastewater purification materials [17]. TiO_2 has three crystalline forms of anatase, rutile and brookite. Among them, anatase possesses the best photocatalytic properties. TiO_2 can produce pairs of electrons and holes by absorbing ultraviolet radiation. The electron of the valence band of TiO_2 becomes excited when illuminated by light. The excess energy of this excited electron promotes the electron to the conduction band of TiO_2 therefore creating the negative-electron (e^-) and positive-hole (h^+) pair. The positive-hole of TiO_2 breaks apart the H_2O molecule to form $^{\bullet}OH$ and H_2. The e^- reacts with O_2 molecule to form super oxide anion and this cycle continues until light is available [18]. Using a support can increase the photocatalytic reaction of TiO_2 through immobilization of the TiO_2 photocatalyst, increasing the illuminated specific catalyst area and increasing the adsorption capacity and surface area of the photocatalyst. Previous works has been attempted to use the adsorbent such as silica [19,20], alumina [21,22], zeolite [23,24] and activated carbon [25,26]. In the recent works, TiO_2 supported activated carbon (AC/TiO_2) has been reported that it exhibits a synergistic effect of its constituents, TiO_2 and AC [27–31]. For example, Song et al. [30] prepared nitrogen-doped TiO_2/magnetic activated carbon (N-TiO_2/MAC) photocatalytic composites. It demonstrated a good photoelectrochemical absorption in the visible light region when used as the catalyst in salicylic acid (SA) oxidation. It obeyed a pseudo-first-order reaction rate with an optimized photoelectrochemical reaction rate constant of 0.0093 min^{-1} (SA, initial concentration = 50 mg/L), much higher 0.0011 min^{-1} for the individual use of the composite in photocatalysis. Meng et al. [27] synthesized TiO_2 nanoparticles-loaded activated carbon fibers (TiO_2/ACF) by a hydrothermal method. They observed improved adsorption and photocatalytic activity of the composite toward Rhodamine B (RhB) as compared with that of ACF. In another work, Vishnuganth et al. [31] applied the TiO_2 coated granular activated carbon (GAC/TiO_2) for photocatalytic degradation of carbofuran (CBF) in a batch-mode reaction. They obtained an optimized performance of the photocatalyst at an initial concentration of 50 mg/L and 100 mg/L at a contact time of 90 and 120 min, respectively. Moreover, adsorption equilibrium data were fitted by a modified Langmuir-Hinshelwood (L-H) model while the observed kinetics demonstrated that the surface reaction was the rate limiting step in the GAC/TiO_2 catalyzed photodegradation of CBF, when it modeled by a pseudo first-order reaction. Zhang et al. [32] developed nanoTiO_2-supported activated carbon (TiO_2/AC) for the microwave (MW) degradation of an azo dye, methyl orange (MO), selected as a model contaminant in aqueous solution. The results showed that the supported TiO_2 on AC could be excited resulting in the production of hydroxyl radical ($^{\bullet}OH$) in aqueous solution under MW irradiation, which significantly enhanced the performance of AC/MW process for the degradation of MO. Also, the supported-TiO_2/AC displayed higher catalytic activity than AC alone under MW irradiation. By comparison, the supported-TiO_2/AC/MW process exhibited several advantages, including high degradation rate, short irradiation time, no residual intermediates and no secondary pollution. Nasirian et al. [33] developed a photocatalyst by doping transition metals, especially noble metals such as Ag, onto the original TiO_2 for the treatment of two azo dyes, Congo Red (CR) and Methyl Orange (MO) under the UV-vis irradiation. In their study, first Ag-doped TiO_2 was prepared and then, a composite of Fe_2O_3/TiO_2 was synthesized in different mass ratios. They concluded that silver doped TiO_2 increases the degradation of MO (12.2%) and CR (14.5%) compared to that of the bare TiO_2. Furthermore, they demonstrated that degradation efficiency of MO and CR increases by applying composite photocatalyst of Fe_2O_3/TiO_2 in the range of 28.9 and 25.1%, respectively, compared to that of the bare TiO_2.

In the present work, for a first time the removal of CR dye by TiO_2 nanoparticles loaded activated carbon (AC/TiO_2) was investigated in a photocatalytic reactor. Nanocrystalline AC/TiO_2 was prepared by sol-gel method in order to achieve in anatase phase having the best photocatalytic properties. Comparing the results, removal efficiencies of CR by AC, AC/TiO_2 and the composite under UV irradiation (AC/TiO_2/UV) have been studied. The adsorption kinetics and isotherm models for CR removal were also investigated.

2. Experimental

2.1. Materials

The dye, Congo red (CR) (C.I. No. 22120, Direct red28) is the sodium salt of benzidinediazo-bis-1-naphthylamine-4-sulfonicacid having a chemical formula $C_{32}H_{22}N_6Na_2O_6S_2$ and molecular mass 696.66 g/mol, used in this study was supplied by Sigma–Aldrich (Milwaukee, WI, USA). The molecular structure of Congo red is shown in Fig. 1. HCl and NaOH were used to adjust pH, and along with all the used materials in the synthesis process of AC/TiO_2 were bought from Merck Company (Darmstadt, Germany).

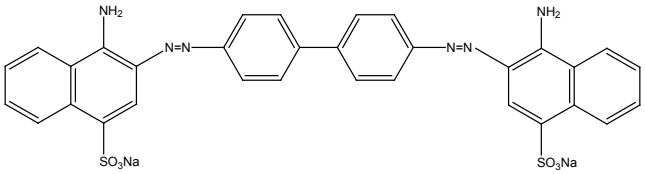

Fig. 1. Molecular structure of CR dye.

2.2. Synthesis of AC/TiO_2 nanocomposite

In this study, AC/TiO_2 nanophotocatalyst was synthesized from titanium tetra-isopropoxide ($C_{12}H_{28}O_4Ti$) by sol–gel method in the presence of AC and mechanical mill. Before using the bought carbon, it is necessary that its surface being activated. So, carbon was washed by menthol ($C_{10}H_{20}O$) to clean its surface from dust. Then, in order to activate it, modifying its surface and finally increasing the adsorbing capacity, it was washed by 0.1 molar nitric acid and distilled water. After filtration, it was dried in an oven at 80°C to activate through heating the powders and also to attain the smooth and uniform activated carbon. The process of nanocomposite synthesis is shown in Fig. 2. Under constant stirring condition, 1 g AC was suspended in 2 mL titanium iso-propoxide. Then, 20 mL isopropyl alcohol (C_3H_7OH) was added and was stirred for 1 h. The AC/TiO_2 was dried by incubation at 120°C for 1 h and then calcined at 400°C for 1 h [29,32].

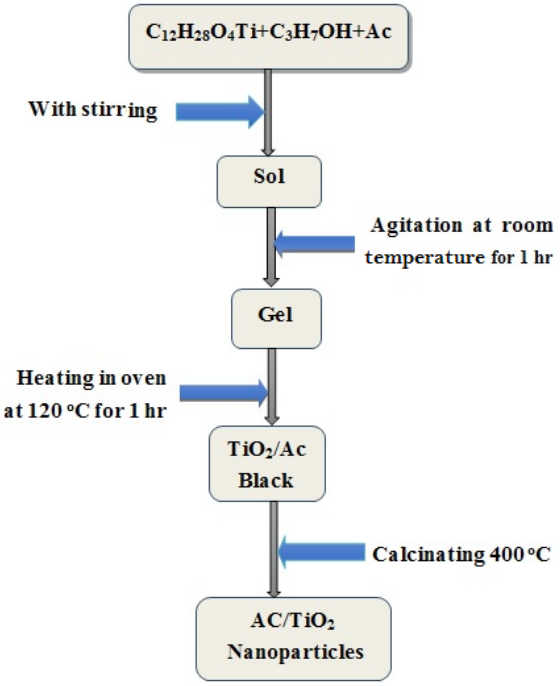

Fig. 2. Synthesis process of AC/TiO_2 nanocomposites.

2.3. Characterization of synthesized AC/TiO_2 nanocomposites

Scanning electron microscopy (SEM, Philips XL30, Eindhoven, Netherlands), XRD (Bruker Analytical X-ray Systems, Berlin, Germany) and FTIR (Thermo Nicolet Nexus 870 FT-IR, Madison, USA) analyses were done on the synthesized AC/TiO_2 nanocomposites. Also, the nanoparticle sizes were calculated by Debye-Scherrer's equation through the following equation [34]:

$$D = \frac{K\lambda}{\beta\cos\theta} \quad (1)$$

where D is the crystal size (nm), l is wave length of the used X ray beams, β is the angle in which the longest peak was appeared, θ is the angle between UV radiation and plate, and K is a constant.

2.4. Photocatalytic degradation of CR dye using synthesized nanocomposites

At first, some samples of waste water with specified concentration of CR in deionized water were prepared. One at the time method was used in the experiments. All prepared samples contain 1 L of CR solution. Then, different amounts of AC/TiO_2 nanophotocatalyst were added to the solution. The solutions were mixed in darkness for 5 minutes to investigate the adsorption of dye by nanocomposites. Next, in order to investigate the catalytic degradation of CR dye, an experimental glassy photocatalytic-reactor was constructed with the capacity of 1 L and a 15 W UV lamp as a radiation source. The solutions containing synthesized nanocomposites were taken under UV radiation for 120 min. Afterwards, sampling was done in 5 min intervals to investigate the amount of decomposed dye. At last, the samples were put in a centrifuge with a speed of 400 rpm to separate nanoparticles from the solutions. The concentration of CR in each aqueous solution was measured on an UV–vis laboratory spectrophotometer (Hach DR 5000, Loveland, USA). Since maximum wave length (λ_{max}) is a key index in qualitative and quantitative measurements, so adsorption spectrum for the CR dye solution was plotted in Fig. 3 in the wave length range of 400–700 nm. As can be seen, λ_{max} was happened at about 499 nm. So, the concentration of CR in the solution was measured at λ_{max} = 499 nm.

The percentage removal of CR dye can be calculated from the following equation [35]:

$$R_t(\%) = \frac{C_o - C_t}{C_t} \times 100 \quad (2)$$

where R_t is the percentage removal of dye at time t, C_0 is the concentration of CR at initial time and C_t is the concentration of CR at time t. The adsorption capacity of dyes was then calculated using the relation $q = VDC/m$, where V was the volume of the liquid phase, m was the mass of the adsorbent, and DC was the difference between the initial and final concentration of dye in solution [36]. For the experiments of adsorption kinetics, the amounts of dye adsorption were determined by analyzing the solution at appropriate time intervals at room temperature.

3. Results and discussion

3.1. Characterization results

Fig. 4 shows the XRD pattern of the AC/TiO_2 nanocomposites. By the adaption of this pattern with standard card

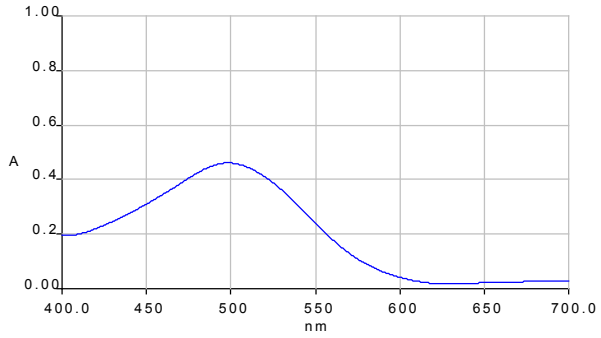

Fig. 3. Adsorption spectrum for the CR dye solution.

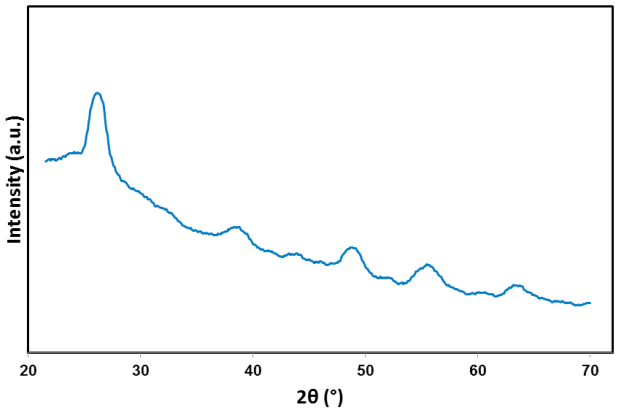

Fig. 4. XRD pattern of AC/TiO_2 nanocomposites calcined at 400°C.

(JCPDS file No. 21-1272), it became clear that this nanocomposite complies the anatase form of the TiO_2 crystals. As stated by other researches [37,38], no anatase phase was detected by XRD for the AC. The anatase phase of TiO_2 is identified at 2θ of 25.4°, 38.1°, 48.2°, 53.9°, 55.1° and 62.2 [39,40]. Also, no extra phases can be seen in this pattern. Therefore, it can be stated that no chemical reaction was occurred between TiO_2 and AC. In addition, the highest crystallite size of TiO_2 in nanocomposite which is calculated by Debye-Scherrer's equation (2θ = 25.4°) is about 10 nm. Some lower crystal values corresponding to the other peaks of TiO_2/AC nanocomposite can also be calculated that attribute to presence of decomposition products of AC into the crystalline structure of TiO_2 [41].

In order to investigate the microstructure and morphology of the synthesized nanocomposites, SEM was done. Figs. 5a–c show the SEM images from the synthesized samples at different scales. The SEM images of AC/TiO_2 show that the activated carbon was homogeneously covered with TiO_2 nanoparticles and the AC surface was coated completely with a TiO_2 film. A high level of particle agglomeration was also observed in the SEM images that can be related to the very fine and nano sized dimensions of these nanocomposite particles. Nanosized dimensions of these particles provide high surface area that cause high surface energy which turns a lower particle instability. So, to decrease the surface energy level and increase their stability,

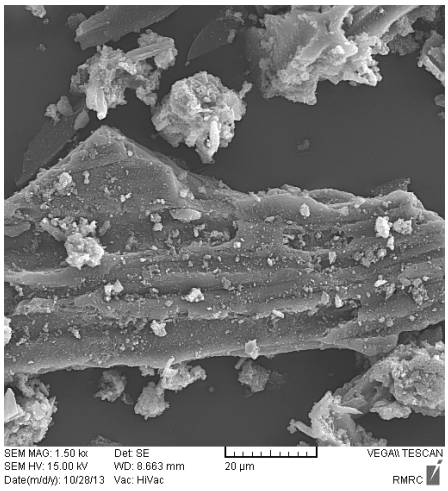

(a)

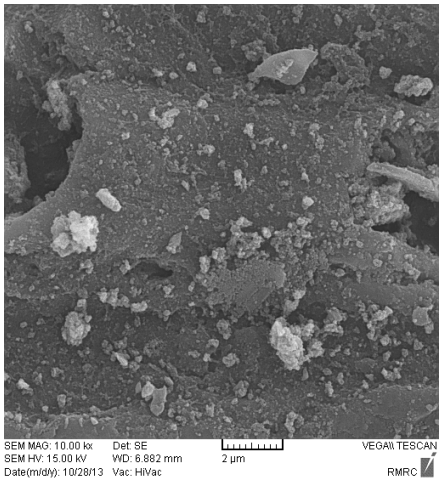

(b)

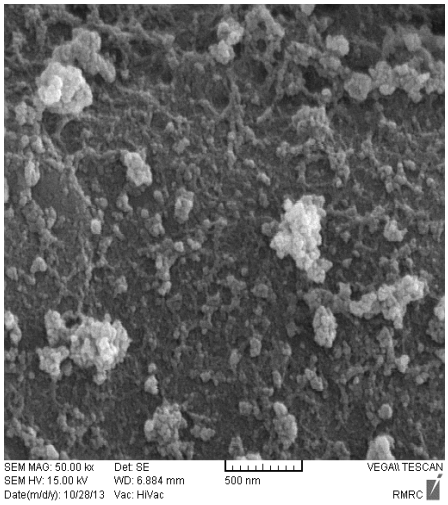

(c)

Fig. 5. SEM images of AC/TiO_2 calcined at 400°C at different magnification orders: (a) 1500, (b) 10,000 and (c) 50,000.

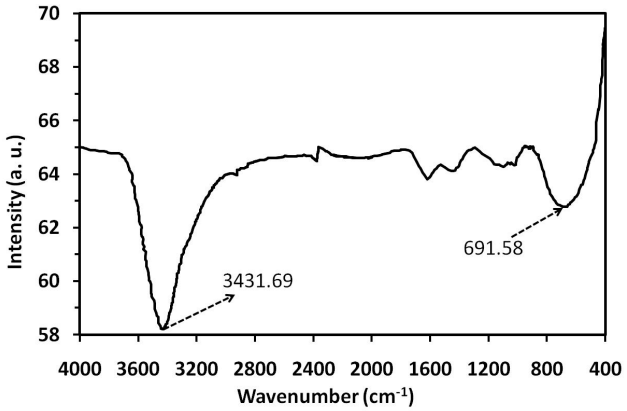

Fig. 6. FTIR spectrum of AC/TiO_2 calcined at 400°C.

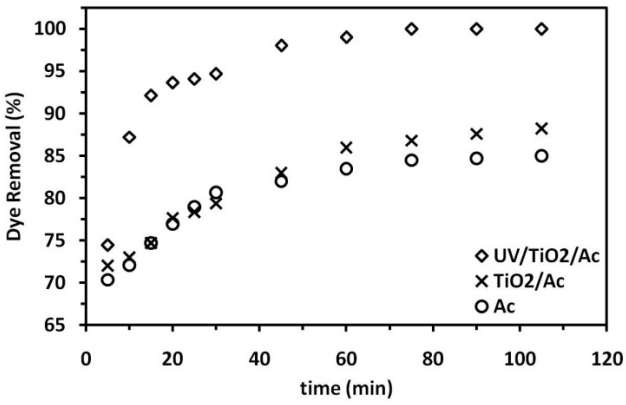

Fig. 7. Effect of UV irradiation on the removal of CR dye at the condition of C_o = 20 mg/L, T = 30°C, pH = 5 and adsorbent dosage = 1 g.

the particles adsorb each other and make some agglomerations which lead to decrease the surface energy, and hence, the more stability [40,42].

In order to investigate the surface properties of AC/TiO_2 nanophoto-catalyst, FTIR spectroscopy was done. Fig. 6 shows the FTIR spectrum of the nanocomposite in the wavenumber ranging from 400–4000 cm^{-1}. An absorption band occurred in a wavenumber of 691.58 cm^{-1} represents for Ti-O bonds. TiO_2 absorption bands overlap with the corresponding bands of the activated carbon, leading to be a decrease in their intensities. The absorption bands related to H–C groups can be seen in the range of 900–950 cm^{-1}. In the wavenumber of 3431.69 cm^{-1} vibrations of hydroxyl (O-H) groups appeared [43]. The vibrations correspond to carbon structure of nanocomposite can be observed in the wavenumber of 800 to 3000 cm^{-1}. The band at 1630 cm^{-1} could be ascribed to the stretching vibration of H-O-H bond from the adsorbed H_2O at the catalyst surface [30]. While the broad band below 700 cm^{-1} is attributed to the existence of Ti-O-Ti bonds [44].

3.2. Parametric study on the removal of CR dye

To evaluate the synthesized AC/TiO_2 nanophoto-composite, the effects of different parameters on the removal of CR dye were investigated.

3.2.1. Effect of UV irradiation

The effect of UV irradiation on the performance of synthesized nanocomposite in dye removal was investigated. For a better comparison, the data of pristine AC was also shown in Fig. 7. The results obviously show that the CR dye degrades in a shorter time with a more efficiency in the presence of UV, which is denoted by the AC/TiO_2/UV, in comparison with two other adsorption data. The main reason is quick production of hydroxyl radicals (•OH) through the UV irradiation on the nanocatalyst. Hydroxyl radicals are the main agent in decomposition of CR dye. It was considered that under UV irradiation some "hot spots" may be generated on the surface of AC due to its non-uniformity. The organic pollutants could be adsorbed and then degraded by these "hot spots". The supported TiO_2 can absorb the heat energy of "hot spots" on the surface of AC under UV irradiation and could be excited to generate electron-hole pairs to form hydroxyl radicals (•OH) in aqueous solution, which can non-selectively attack organic contaminants [45]. Also, the catalytic activities of the supported TiO_2/AC and AC alone were compared. The results showed that the supported-TiO_2 significantly enhanced the AC degradation kinetics and the supported-TiO_2/AC displayed better catalytic activity under UV irradiation.

3.2.2. Effect of pH

In the adsorption processes of waste water, pH value is one of the key factors in process controlling. So in this study the effect of pH on degradation of CR dye in the photocatalytic-reactor under UV irradiation was examined at pH values of 3, 5, 7 and 9. As it is shown in Fig. 8, the adsorption efficiency could increase in acidic conditions (the lower pH). At lower pH, active sites of AC/TiO_2 surface which contain different polar hydroxyl and carboxyl groups are protonated, and so the surface is positively charged. This positive charge, and the growth of interaction between different polar agents in pigment and adsorbent, enhances the adsorption. On the other hand, at higher pH, density of negative charge on the adsorbent surface is increased. So, the active sites of the absorbent are in the form of phenoxide and hydroxide groups that increase electrostatic repulsion of negative ions of CR pigments.

3.2.3. Effect of aqueous solution concentration

Fig. 9 shows the effect of initial dye concentration on the removal of CR at different times. The results clearly show that the discoloration efficiency would decrease with increasing the initial dye concentration. In high concentration of CR dye, active sites of the catalyst surface would surround by the negative charges of CR molecules. Moreover, increasing the CR concentration causes to decrease absorption of UV light by these molecules and hence decreases the removal efficiency. It is also possible to produce intermediate substances compete with the original CR dye molecules for degradation.

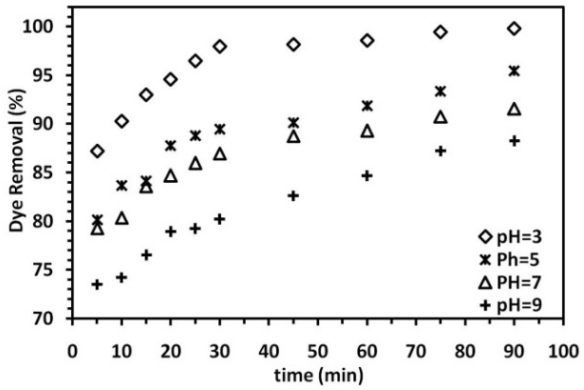

Fig. 8. Effect of pH on the removal of CR dye by AC/TiO_2 nanocomposite under UV irradiation at the condition of C_o = 20 mg/L, T = 30°C and adsorbent dosage = 1 g.

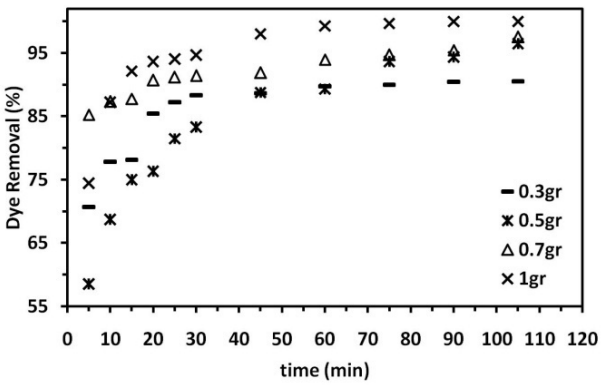

Fig. 10. Effect of adsorbent dosage on the removal of CR dye by AC/TiO_2 nanocomposite under UV irradiation at the condition of C_o = 20 mg/L, T = 30°C and pH = 5.

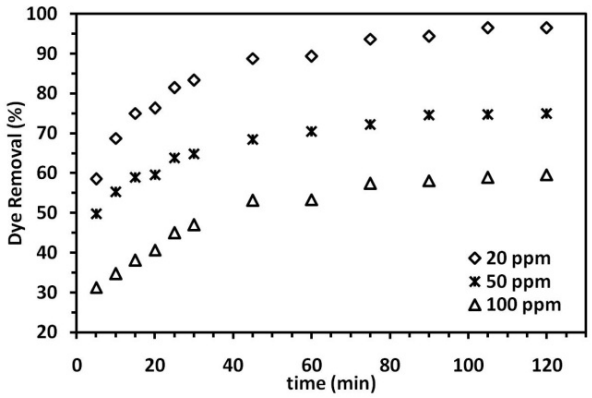

Fig. 9. Effect of solution concentration on the removal of CR dye by AC/TiO_2 nanocomposite under UV radiation at the condition of T = 30°C, pH = 5 and adsorbent dosage = 1 g.

3.2.4. Effect of adsorbent dosage

The amount of catalyst used in the process of dye elimination is an important parameter because it determines the adsorbent capacity for the preliminarily concentrations of pigment solutions. Effect of the AC/TiO_2 photocatalyst dosage on the optical decomposition of pigment in pH = 7 was investigated in the range of 0.3–1 g and the results are shown in Fig. 10. It is obviously shown that with the increment in adsorbent dosage from 0.3 to 1 g, pigment elimination increases from 87.52 to 97.49 %. Due to the increase in the amounts of active sites of photocatalyst surfaces the related electron pairs increase. Thus the hydroxyl and super oxide radicals are increased. It doesn't mean that more catalysts have more effect on optical decomposition, but the truth is that when catalyst concentration exceeds from a specific amount, the rate of decomposition can be reduced due to the reduction of UV penetration in the solution.

3.2.5. Effect of temperature

In order to investigate the effect of temperature on the CR dye removal, the experiments were conducted at temperatures of 30, 40 and 50°C. As can be seen in Fig. 11, the best operating temperature for total pigment removal after 90 min is 50°C. However, in order to better controlling the reactor performance, the lower temperature of 30°C, with no more considerable difference in percentage removal as compared to 50°C, is selected as the best operating condition in this situation.

It was experienced that kinetic rate of all chemical reactions, either exothermic or endothermic, is increased with temperature. Rate of some reactions is extremely increased upon temperature that it becomes out of control and even it can be exploded. At high temperatures, the reactant molecules have more collisions because of their more kinetic energy. Accordingly, they can support more activation energy and further changes to activated complex.

3.3. Mechanisms of CR degradation on UV/TiO_2/AC

Basic principle of TiO_2 photocatalysis depends on the creation of an electron–hole pair after the light absorption with energy equal to or greater than the band gap energy of TiO_2 photocatalyst. These photogenerated charge carriers are responsible for photocatalytic activity of TiO_2 to degrade pollutants. However, the major problem of TiO_2 is its wide band gap such as 3.2 and 3.0 eV for anatase and rutile phases respectively. This makes it active under only UV light irradiation and therefore, no performance under visible light [46]. Fig. 12 demonstrates a schematic mechanism of TiO_2 photocatalysis on the carbonaceous support. AC particles can strongly absorb UV energy and then generate many "hot spots" on their surfaces [47]. The organic pollutants around the "hot spots" can be decomposed in the presence of dissolved oxygen in water. It is considered to be a process being similar to combustion oxidation. The temperature of "hot spot" on the surface of AC under UV irradiation in water medium can achieve 1200°C or more. It results in significant increase in the number of activated sites and brings many holes to produce hydroxyl radical (•OH) on the surface of semiconductor catalyst in the solution. The supported-TiO_2 is able to absorb the heat energy of "hot spots" and can be excited to generate the electron-hole pairs that would react with O_2 and H_2O to form •OH and

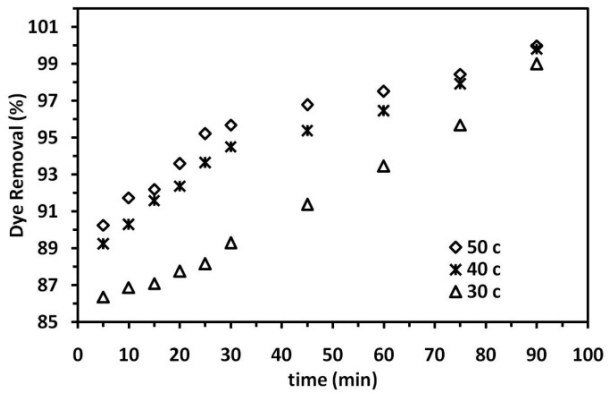

Fig. 11. Effect of temperature on the removal of CR dye by AC/TiO_2 nanocomposite under UV irradiation at the condition of C_o = 20 mg/L, pH = 5 and adsorbent dosage = 1 g.

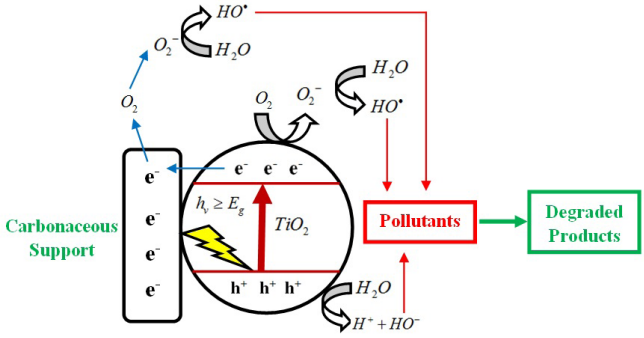

Fig. 12. A schematic mechanism of TiO_2 photocatalysis on the carbonaceous support.

superoxide radical anion $O_2^{\bullet-}$. Finally, the •OH can also yield $O_2^{\bullet-}$ through a series of chemical reactions [48]. Thus, the degradation rates can be increased. In brief, supported-TiO_2/AC can be adopted as a catalyst to help produce more activated sites on the surface of AC and much •OH radicals in the solution under UV irradiation, which is expected to increase the rates of degradation of recalcitrant organic contaminants and reaction intermediates formed.

3.4. Kinetic and adsorption isotherm models

3.4.1. Kinetic models

In order to investigate the kinetic behavior of CR dye removal by AC/TiO_2 nanophotocatalyst, different kinetic models are applied to examine the controlling mechanism of adsorption process. The proposed kinetic models are selected based on the frequently used ones in the literature for the range of adsorption capacity of adsorbent. In this study, the respective experimental data of dye removal with progress in time were fitted to various kinetic models namely pseudo-first-order kinetic model [Eq. (3)], pseudo-second-order kinetic model [Eq. (4)], Elovich [Eq. (5)] and intraparticle diffusion models.

$$\log(q_e - q_t) = \log q_e - \frac{k_1}{2.303}t \tag{3}$$

$$\frac{t}{q_t} = \frac{1}{k_2 q_e^{\,2}} + \frac{1}{q_e}t \tag{4}$$

$$q_t = \frac{1}{\beta}\ln(\alpha\beta) + \frac{1}{\beta}\ln(t) \tag{5}$$

where q_e and q_t refer to the amounts of CR dye adsorbed (mg g^{-1}) at equilibrium and at any time, t (min), respectively. Also, k_1 is the equilibrium rate constant of the pseudo-first-order sorption (min^{-1}). k_2 is the equilibrium rate constant of the pseudo-second-order adsorption (g mg^{-1} min^{-1}), α is the primary adsorption rate (mg g^{-1} min^{-1}) and β is the desorption constant (g mg^{-1}). The results of kinetic investigations are shown in Table 1.

The values of R^2 and/or the agreement between theoretical and experimental q_e indicate the suitability of the model (Table 1). R^2 values for pseudo-second-order kinetic model were found to be closer to 1.0 and the calculated q_e values are also very close to those of experimental data. This indicates that the CR dye adsorption on AC/TiO_2 nanophotocatalyst obeys the pseudo-second-order kinetic model. The second-order rate constants were used to calculate the initial sorption rate (h), given by Eq. (6), and the obtained values are presented in Table 1.

$$h = k_2 q_e^{\,2} \tag{6}$$

k_2 and the equilibrium adsorption value (q_e) were measured from the slope and intercept of the plot t/q_t versus t [49]. The Elovich model constants obtained from the slope and intercept of an straight line fitted to the experimental data [50]. The linear relation of initial dye concentration with removal rate fails when pore diffusion is the predominant stage and limits the adsorption process. The target compound (pollutant) presents in the bulk transfer to the solid phase through intraparticle diffusion/transport process. This stage is generally known as rate-limiting step, especially in rapidly stirred batch processes [51]. Therefore, the possibility of this model for interpretation of experimental data was explored according to its well-known equation:

$$q_t = k_{dif} t^{1/2} + C \tag{7}$$

where C (mg g^{-1}) is the intercept and k_{dif} (mg g^{-1} $min^{-1/2}$) is the intraparticle diffusion rate constant. The values of q_t were found to be linearly correlated with the values of $t^{1/2}$ with the rate constant k_{dif} The values were directly evaluated from the slope of the regression line and presented in Table 1. The values of intercept C provide information about the thickness of the boundary layer and the external mass transfer resistance. The constant C was found to be higher for AC adsorbent in respect to AC/TiO_2 nanocomposite. This change in the C values belongs to increase in thickness of the boundary layer and decrease in the chance of the external mass transfer and subsequently prominent increase in the amount of internal mass transfer. The high value of R^2 for AC in comparison with AC/TiO_2 confirms either the suitability of this model for AC and the fact that the rate-limiting step is the intraparticle diffusion process.

Table 1
The kinetic parameters of CR removal by AC and AC/TiO_2 nanophotocatalyst at conditions of pH = 5, T = 30°C, C_o = 20 mg/L, 400 rpm, AC dosage = 0.1 g and AC/TiO_2 dosage = 1 g

Models	Parameters, unit	Adsorbent	
		AC	AC/TiO_2
Pseudo-first order kinetic model:	k_1, min^{-1}	0.026	0.049
$\log(q_e - q_t) = \log(q_e) - \left(\frac{k_1}{2.303}\right)t$	$q_e(calc)$, mg g^{-1}	10.60	4.51
	R^2	0.920	0.957
Pseudo-second order kinetic model:	k_2, g mg^{-1} min^{-1}	0.008	0.025
$dq_t / dt = k_2(q_e - q_t)^2$	$q_e(calc)$, mg g^{-1}	43.48	20.37
	R^2	0.998	0.999
	h, mg g^{-1} min^{-1}	14.22	10.36
Intraparticle diffusion model:	k_{dif}, mg g^{-1} $min^{-1/2}$	1.113	0.545
$q_t = k_{dif}t^{1/2} + C$	C, mg g^{-1}	32.184	15.479
	R^2	0.9485	0.7309
Elovich model:	α, mg g^{-1} min^{-1}	107274.6	9246.9
$q_t = \frac{1}{\beta}\ln(\alpha\beta) + \frac{1}{\beta}\ln(t)$	β, g mg^{-1}	0.360	0.645
	R^2	0.869	0.869
Experimental data	q_e(exp), mg g^{-1}	42.20	19.93

3.4.2. Adsorption isotherm models

The equilibrium isotherm of a specific adsorbent demonstrates its adsorptive characteristics and is very significant for design and optimization of the adsorption processes [52]. Here, various isotherm models were used for the equilibrium sorption of components from their solutions namely Langmuir, Freundlich and Temkin [53]. The correlation coefficient (R^2) for each model was calculated and presented in Table 2. Another important criterion for evaluating the applicability of the model can be obtained from the error analysis, introducing the parameter c^2 The non-linear chi-square test statistic (c^2) for the best-fit isotherm is calculated by the following equation [54]:

$$\chi^2 = \sum \frac{\left(q_{e,\exp} - q_{e,cal}\right)^2}{q_{e,cal}} \quad (8)$$

where $q_{e,\exp}$ and $q_{e,cal}$ are experimental and calculated adsorption capacity values, respectively. The lower c^2 will result in the better agreement between the model and the experimental data.

3.4.2.1. Langmuir isotherm

The Langmuir adsorption isotherm was used to interpret the CR adsorption by AC adsorbent and AC/TiO_2 nanophotocatalyst from the solution. The Langmuir adsorption isotherm is based on the assumption that adsorption takes place on homogeneous surface [55]. The Langmuir equation is given by following equation:

$$\frac{C_e}{q_e} = \frac{1}{K_a Q_m} + \frac{C_e}{Q_m} \quad (9)$$

where Q_m (mg/g) is the maximum amount of dye per unit weight of adsorbent for complete monolayer coverage and K_a is Langmuir adsorption constant in L/mg. Values of Q_m and K_a are determined from the linear regression plot of C_e/q_e vs. C_e (Table 2). Hence it may be concluded that Langmuir isotherm is the best isotherm to predict the adsorption of CR dye over AC/TiO_2 nanophotocatalyst. A significant correlation coefficient (R^2 = 0.997) indicates a good fit to the Langmuir equation. The necessary feature of the Langmuir adsorption isotherm is a separation factor which is expressed by R_L, a dimensionless constant. It can be calculated by the following equation:

$$R_L = 1/(1 + K_a C_0) \quad (10)$$

where C_0 (mg/L) is the initial adsorbate concentration and K_a (L mg^{-1}) is the Langmuir constant. The value of R_L (separation factor) shows the shape of the isotherm to be either unfavorable ($R_L > 1$), linear ($R_L = 1$), favorable ($0 < R_L < 1$) or irreversible ($R_L = 0$). R_L values between 0 and 1 show favorable adsorption of CR onto AC adsorbent and AC/TiO_2 nanophotocatalyst (Table 2).

3.4.2.2. Freundlich isotherm

For heterogeneous surface energy systems the well-known Freundlich isotherm is often used [56]. The heat of adsorption reduces significantly with increasing the extent of adsorption. If the decline in the heat of adsorption is logarithmic, it implies that adsorption sites are distributed exponentially with respect to an adsorption energy which differs between groups of adsorption sites. The linearized Freundlich equation is given as:

$$\ln q_e = \ln K_F + (1/n)\ln C_e \quad (11)$$

where K_F ($mg^{1-1/n}L^{1/n}g^{-1}$) is the Freundlich adsorption equilibrium constant which indicates the adsorption capacity and n is a characteristic coefficient relating to adsorption

Table 2
Isotherm parameters for CR removal by AC and AC/TiO_2 nanophotocatalyst at conditions of pH = 5, T = 30°C, C_o = 20 mg/L, 400 rpm, AC dosage = 0.1 g and AC/TiO_2 dosage =1 g

Isotherm	Equation	Parameters	Adsorbent	
			AC	AC/TiO_2
Langmuir	$C_e / q_e = 1 / K_a Q_m + C_e / Q_m$	Q_m ($mg\ g^{-1}$)	97.09	32.15
		K_a ($L\ mg^{-1}$)	0.183	2.488
		R_L	0.098–0.353	0.007–0.038
		χ^2	12.02	25.16
		R^2	0.908	0.997
Freundlich	$\ln q_e = \ln K_F + (1/n) \ln C_e$	$1/n$	0.465	0.170
		K_F ($mg^{1-1/n} L^{1/n} g^{-1}$)	20.71	20.48
		χ^2	12.80	1.44
		R^2	0.682	0.906
Temkin	$q_e = \beta_1 \ln K_T + \beta_1 \ln C_e$	β_1	20.74	3.30
		K_T ($L\ mg^{-1}$)	2.117	866.233
		χ^2	152.22	0.67
		R^2	0.828	0.989

intensity. K_F and *1/n* were obtained from the intercept and slope of the plot ln q_e vs. ln C_e. K_F shows information about the bonding energy and the adsorption or distribution coefficient. It represents the quantity of dye adsorbed onto the adsorbent. As can be seen in Table 2, K_F for both AC and AC/TiO_2 adsorbents is almost the same. *1/n* shows adsorption intensity of dye onto the adsorbent (surface heterogeneity). It will be closer to zero as the heterogeneity of surface increases (*1/n* < 1 indicates normal Langmuir isotherm while *1/n* > 1 indicates bi-mechanism and cooperative adsorption). It was generally accepted that under a constant temperature, the *n* values increased with decreasing adsorption energy, that the higher *n* numbers show and support, the strong adsorption intensity. *n* > 1 illustrates favorable adsorption and vice versa. So, the results of Table 2 show that adsorption energy of AC/TiO_2 is lower than that of AC adsorbent.

3.4.2.3. Temkin isotherm

The Temkin isotherm contains a factor that explicitly takes into the account adsorbing species–adsorbent interactions. Temkin isotherm derivation assumes that the fall in the heat of sorption is linear rather than logarithmic, as implied in the Freundlich equation [57,58]. The Temkin isotherm model was presented in linear form as follows:

$$q_e = \beta_1 \ln K_T + \beta_1 \ln C_e \quad (12)$$

where $\beta_1 = RT / b$ (the constant β_1 is related to the heat of adsorption), *T* is the absolute temperature (Kelvin) and *R* is the universal gas constant (= 8.314 J·(mol K)$^{-1}$). K_T is the equilibrium binding constant (L/mol) correspond to the maximum binding energy. A plot of q_e versus ln C_e gives the isotherm constants β_1 and K_T from the slope and intercept, respectively.

The calculated values of Temkin parameters are given in Table 2. The non-linear correlation coefficient (R^2) and c^2 were obtained and also shown in Table 2. It was found that the higher R^2 and smaller c^2 values of the Temkin isotherm compared to the similar values of other applied models confirm the high efficiency of the Temkin isotherm to represent the experimental data for AC/TiO_2 nanocomposite. According to c^2, as a significant criterion, the most applicable model is Temkin model for AC/TiO_2 nanocomposite. On the other hand, the most applicable model for AC adsorbent is Langmuir model.

4. Conclusions

AC/TiO_2 nanophotocatalyst was prepared at 400°C using a simple and effective sol-gel method involving a titanium tetra-isopropoxide precursor and isopropanol. The nanocomposite was characterized by XRD, SEM and FTIR. The results showed that the TiO_2 nanoparticles have anatase phase with 10 nm particle diameter. Furthermore parametric studies were conducted at the conditions of C_0 = 20 mg/L, T = 30°C, pH = 5 and adsorbent dosage = 1 g for synthesized AC/TiO_2 and the results clearly showed that the maximum efficiency of CR removal was obtained in the present of UV irradiation on AC/TiO_2 nanocomposite at pH = 3, dye concentration of 20 ppm, adsorbent dosage of 1 g and temperature of 50°C. The kinetics of CR dye adsorption on AC and AC/TiO_2 nanophotocatalyst follows the pseudo-second-order model. The adsorption isotherms of CR dye from the aqueous solution onto the AC and AC/TiO_2 were also determined. The experimental isotherms were appropriately described by the Langmuir and Temkin models for AC and AC/TiO_2 adsorbents, respectively.

References

[1] M. Ghaedi, F. Karimi, B. Barazesh, R. Sahraei, A. Daneshfar, Removal of Reactive Orange 12 from aqueous solutions by adsorption on tin sulfide nanoparticle loaded on activated carbon, J. Ind. Eng. Chem., 19 (2013) 756–763.

[2] T. Robinson, G. McMullan, R. Marchant, P. Nigam, Remediation of dyes in textile effluent: a critical review on current treatment technologies with a proposed alternative, Bioresour. Technol., 77 (2001) 247–255.
[3] I.L. Finar, Organic Chemistry: The Fundamental Princiles, 6th ed., Addison Wesley Longman Ltd, England, 1986.
[4] C. Namasivayam, D. Kavitha, Removal of Congo Red from water by adsorption onto activated carbon prepared from coir pith, an agricultural solid waste, Dyes Pigments, 54 (2002) 47–58.
[5] A.B. dos Santos, I.A.E. Bisschops, F.J. Cervantes, J.B. van Lier, Effect of different redox mediators during thermophilic azo dye reduction by anaerobic granular sludge and comparative study between mesophilic (30°C) and thermophilic (55°C) treatments for decolourisation of textile wastewaters, Chemosphere, 55 (2004) 1149–1157.
[6] V. Shenai, Azo dyes on textiles vs German ban, an objective assessment, Chem. Weekly, 12 (1996) 33–44.
[7] D. Brown, Effects of colorants in the aquatic environment, Ecotoxicol. Environ. Safety, 13 (1987) 139–147.
[8] F. Gähr, F. Hermanutz, W. Oppermann, Ozonation – an important technique to comply with new German laws for textile wastewater treatment, Water Sci. Technol., 30 (1994) 255–263.
[9] K.-C. Chen, J.-Y. Wu, C.-C. Huang, Y.-M. Liang, S.-C.J. Hwang, Decolorization of azo dye using PVA-immobilized microorganisms, J. Biotechnol., 101 (2003) 241–252.
[10] A. Mittal, J. Mittal, A. Malviya, D. Kaur, V.K. Gupta, Decoloration treatment of a hazardous triarylmethane dye, Light Green SF (Yellowish) by waste material adsorbents, J. Colloid Interface Sci., 342 (2010) 518–527.
[11] R. Jain, S. Sikarwar, Adsorptive removal of erythrosine dye onto activated low cost de-oiled mustard, J. Hazard. Mater., 164 (2009) 627–633.
[12] Y. Zhu, P. Kolar, Adsorptive removal of p-cresol using coconut shell-activated char, J. Environ. Chem. Eng., 2 (2014) 2050–2058.
[13] M.B. Ahmed, J.L. Zhou, H.H. Ngo, W. Guo, Adsorptive removal of antibiotics from water and wastewater: Progress and challenges, Sci. Total Environ., 532 (2015) 112–126.
[14] M. Wawrzkiewicz, M. Wiśniewska, V.M. Gun'ko, V.I. Zarko, Adsorptive removal of acid, reactive and direct dyes from aqueous solutions and wastewater using mixed silica–alumina oxide, Powder Technol., 278 (2015) 306–315.
[15] M. Ghaedi, Comparison of cadmium hydroxide nanowires and silver nanoparticles loaded on activated carbon as new adsorbents for efficient removal of Sunset yellow: Kinetics and equilibrium study, Spectrochim. Acta Part A: Molec. Biomolec. Spectrosc., 94 (2012) 346–351.
[16] F. Haghseresht, S. Nouri, J.J. Finnerty, G.Q. Lu, Effects of surface chemistry on aromatic compound adsorption from dilute aqueous solutions by activated carbon, J. Phys. Chem. B, 106 (2002) 10935–10943.
[17] W. Wang, C.G. Silva, J.L. Faria, Photocatalytic degradation of Chromotrope 2R using nanocrystalline TiO_2/activated-carbon composite catalysts, Appl. Catal. B: Environ., 70 (2007) 470–478.
[18] H. Choi, E. Stathatos, D.D. Dionysiou, Sol–gel preparation of mesoporous photocatalytic TiO_2 films and TiO_2/Al_2O_3 composite membranes for environmental applications, Appl. Catal. B: Environ., 63 (2006) 60–67.
[19] J. Qiu, Z. Wang, H. Li, L. Xu, J. Peng, M. Zhai, C. Yang, J. Li, G. Wei, Adsorption of Cr(VI) using silica-based adsorbent prepared by radiation-induced grafting, J. Hazard. Mater., 166 (2009) 270–276.
[20] T. Yokoi, Y. Kubota, T. Tatsumi, Amino-functionalized mesoporous silica as base catalyst and adsorbent, Appl. Catal. A: General, 421–422 (2012) 14–37.
[21] M. Karthikeyan, K.K. Satheesh Kumar, K.P. Elango, Conducting polymer/alumina composites as viable adsorbents for the removal of fluoride ions from aqueous solution, J. Fluorine Chem., 130 (2009) 894–901.
[22] M.E. Mahmoud, M.M. Osman, O.F. Hafez, A.H. Hegazi, E. Elmelegy, Removal and preconcentration of lead (II) and other heavy metals from water by alumina adsorbents developed by surface-adsorbed-dithizone, Desalination, 251 (2010) 123–130.
[23] R.I. Yousef, B. El-Eswed, A.a.H. Al-Muhtaseb, Adsorption characteristics of natural zeolites as solid adsorbents for phenol removal from aqueous solutions: Kinetics, mechanism, and thermodynamics studies, Chem. Eng. J., 171 (2011) 1143–1149.
[24] L. Damjanović, V. Rakić, V. Rac, D. Stošić, A. Auroux, The investigation of phenol removal from aqueous solutions by zeolites as solid adsorbents, J. Hazard. Mater., 184 (2010) 477–484.
[25] F. Raposo, M.A. De La Rubia, R. Borja, Methylene blue number as useful indicator to evaluate the adsorptive capacity of granular activated carbon in batch mode: Influence of adsorbate/adsorbent mass ratio and particle size, J. Hazard. Mater., 165 (2009) 291–299.
[26] C. Hung-Lung, L. Kuo-Hsiung, C. Shih-Yu, C. Ching-Guan, P. San-De, Dye adsorption on biosolid adsorbents and commercially activated carbon, Dyes Pigments, 75 (2007) 52–59.
[27] H. Meng, W. Hou, X. Xu, J. Xu, X. Zhang, TiO_2-loaded activated carbon fiber: Hydrothermal synthesis, adsorption properties and photo catalytic activity under visible light irradiation, Particuology, 14 (2014) 38–43.
[28] E.-C. Su, B.-S. Huang, C.-C. Liu, M.-Y. Wey, Photocatalytic conversion of simulated EDTA wastewater to hydrogen by pH-resistant Pt/TiO_2–activated carbon photocatalysts, Renew. Energy, 75 (2015) 266–271.
[29] X. Fu, H. Yang, G. Lu, Y. Tu, J. Wu, Improved performance of surface functionalized TiO_2/activated carbon for adsorption–photocatalytic reduction of Cr(VI) in aqueous solution, Mater. Sci. Semicond. Process., 39 (2015) 362–370.
[30] J. Song, X. Wang, J. Huang, J. Ma, X. Wang, H. Wang, R. Ma, P. Xia, J. Zhao, High performance of N-doped TiO_2 magnetic activated carbon composites under visible light illumination: Synthesis and application in three-dimensional photoelectrochemical process, Electrochim. Acta, 222 (2016) 1–11.
[31] M.A. Vishnuganth, N. Remya, M. Kumar, N. Selvaraju, Photocatalytic degradation of carbofuran by TiO_2-coated activated carbon: Model for kinetic, electrical energy per order and economic analysis, J. Environ. Manage., 181 (2016) 201–207.
[32] Z. Zhang, Y. Xu, X. Ma, F. Li, D. Liu, Z. Chen, F. Zhang, D.D. Dionysiou, Microwave degradation of methyl orange dye in aqueous solution in the presence of nano-TiO_2-supported activated carbon (supported-TiO_2/AC/MW), J. Hazard. Mater., 209–210 (2012) 271–277.
[33] M. Nasirian, M. Mehrvar, Modification of TiO_2 to enhance photocatalytic degradation of organics in aqueous solutions, J. Environ. Chem. Eng., 4 (2016) 4072–4082.
[34] K. Pomoni, A. Vomvas, C. Trapalis, Dark conductivity and transient photoconductivity of nanocrystalline undoped and N-doped TiO_2 sol–gel thin films, Thin Solid Films, 516 (2008) 1271–1278.
[35] M.I. Kandah, J.-L. Meunier, Removal of nickel ions from water by multi-walled carbon nanotubes, J. Hazard. Mater., 146 (2007) 283–288.
[36] V. Gómez, M.S. Larrechi, M.P. Callao, Kinetic and adsorption study of acid dye removal using activated carbon, Chemosphere, 69 (2007) 1151–1158.
[37] Z. Ding, X. Hu, P.L. Yue, G.Q. Lu, P.F. Greenfield, Synthesis of anatase TiO_2 supported on porous solids by chemical vapor deposition, Catal. Today, 68 (2001) 173–182.
[38] S.X. Liu, X.Y. Chen, X. Chen, A TiO_2/AC composite photocatalyst with high activity and easy separation prepared by a hydrothermal method, J. Hazard. Mater., 143 (2007) 257–263.
[39] C. Ngamsopasiriskun, S. Charnsethikul, S. Thachepan, A. Songsasen, Removal of phenol in aqueous solution by nanocrystalline Tio_2/activated carbon composite catalyst, Kasetsart J. (Nat. Sci.), 44 (2010) 1176–1182.
[40] C.-C. Wang, J.Y. Ying, Sol–Gel synthesis and hydrothermal processing of anatase and rutile titania nanocrystals, Chem. Mater., 11 (1999) 3113–3120.
[41] A.C. Martins, A.L. Cazetta, O. Pezoti, J.R.B. Souza, T. Zhang, E.J. Pilau, T. Asefa, V.C. Almeida, Sol-gel synthesis of new TiO_2/activated carbon photocatalyst and its application for degradation of tetracycline, Ceramics Int., 43 (2017) 4411–4418.

[42] R. Bacsa, J. Kiwi, T. Ohno, P. Albers, V. Nadtochenko, Preparation, testing and characterization of doped TiO_2 active in the peroxidation of biomolecules under visible light, J. Phys. Chem. B, 109 (2005) 5994–6003.
[43] P. Singh, M.C. Vishnu, K.K. Sharma, A. Borthakur, P. Srivastava, D.B. Pal, D. Tiwary, P.K. Mishra, Photocatalytic degradation of Acid Red dye stuff in the presence of activated carbon-TiO_2 composite and its kinetic enumeration, J. Water Process Eng., 12 (2016) 20–31.
[44] Y. Shao, C. Cao, S. Chen, M. He, J. Fang, J. Chen, X. Li, D. Li, Investigation of nitrogen doped and carbon species decorated TiO_2 with enhanced visible light photocatalytic activity by using chitosan, Appl. Catal. B: Environ., 179 (2015) 344–351.
[45] J. Wang, W. Sun, Z. Zhang, Z. Jiang, X. Wang, R. Xu, R. Li, X. Zhang, Preparation of Fe-doped mixed crystal TiO_2 catalyst and investigation of its sonocatalytic activity during degradation of azo fuchsine under ultrasonic irradiation, J. Colloid Interf. Sci., 320 (2008) 202–209.
[46] O. Carp, C.L. Huisman, A. Reller, Photoinduced reactivity of titanium dioxide, Progr. Solid State Chem., 32 (2004) 33–177.
[47] X. Quan, Y. Zhang, S. Chen, Y. Zhao, F. Yang, Generation of hydroxyl radical in aqueous solution by microwave energy using activated carbon as catalyst and its potential in removal of persistent organic substances, J. Molec. Catal. A: Chemical, 263 (2007) 216–222.
[48] J. Wang, G. Zhang, Z. Zhang, X. Zhang, G. Zhao, F. Wen, Z. Pan, Y. Li, P. Zhang, P. Kang, Investigation on photocatalytic degradation of ethyl violet dyestuff using visible light in the presence of ordinary rutile TiO_2 catalyst doped with upconversion luminescence agent, Water Res., 40 (2006) 2143–2150.
[49] Y.S. Ho, G. McKay, Pseudo-second order model for sorption processes, Process Biochem., 34 (1999) 451–465.
[50] S.H. Chien, W.R. Clayton, Application of Elovich equation to the kinetics of phosphate release and sorption in soils, Soil Sci. Soc. Amer. J., 44 (1980) 265–268.
[51] G. McKay, The adsorption of dyestuffs from aqueous solution using activated carbon: Analytical solution for batch adsorption based on external mass transfer and, Chem. Eng. J., 27 (1983) 187–196.
[52] E. Erdem, G. Çölgeçen, R. Donat, The removal of textile dyes by diatomite earth, J. Colloid Interf. Sci., 282 (2005) 314–319.
[53] A. Dąbrowski, Adsorption - from theory to practice, Adv. Colloid Interf. Sci., 93 (2001) 135–224.
[54] Y.-S. Ho, A.E. Ofomaja, Kinetics and thermodynamics of lead ion sorption on palm kernel fibre from aqueous solution, Process Biochem., 40 (2005) 3455–3461.
[55] A. Rodríguez, J. García, G. Ovejero, M. Mestanza, Adsorption of anionic and cationic dyes on activated carbon from aqueous solutions: Equilibrium and kinetics, J. Hazard. Mater., 172 (2009) 1311–1320.
[56] H. Freundlich, W. Heller, The Adsorption of cis- and trans-Azobenzene, J. Amer. Chem. Soc., 61 (1939) 2228–2230.
[57] X.-s. Wang, Y. Qin, Equilibrium sorption isotherms for of Cu^{2+} on rice bran, Process Biochem., 40 (2005) 677–680.
[58] C. Aharoni, S. Levinson, I. Ravina, D.L. Sparks, Kinetics of soil chemical reactions: relationships between empirical equations and diffusion models, Soil Sci. Soc. Amer. J., 55 (1991) 1307–1312.